ELSEVIER

Polymer 42 (2001) 2449–2454

polymer

www.elsevier.nl/locate/polymer

Electrosynthesis of adherent poly(2-mercaptobenzimidazole) films on brass prepared in nonaqueous solvents

B. Assouli[a,b,*], Z.A. Ait Chikh[a], H. Idrissi[b], A. Srhiri[a]

[a]*Laboratoire d'Electrochimie et des Etudes de Corrosion, Faculté des Sciences, Université IBN Tofail, BP 133, Kénitra, Morocco*
[b]*Laboratoire de Physico-Chimie Industrielle, INSA, Bâtiment 401, Avénue Albert Einstein, 69621 Villeurbanne cedex, France*

Received 17 February 2000; received in revised form 24 June 2000; accepted 31 July 2000

Abstract

The kinetics of the electropolymerization of 2-mercaptobenzimidazole (2-MBI) on a brass substrate in alkaline solution containing methanol was investigated using cyclic polarization, chronoamperometry and electrochemical impedance techniques. The polymeric film was prepared by successive cycles of potential of a Cu–Zn electrode between 0.2 and 2.4 V. During the second cycle, the oxidation peak of the monomer disappears indicating the formation of the insulating film. We have also shown that the monomer oxidation reaction is essentially irreversible and controlled by a diffusion process. The protective effect of the film formed on brass has been studied in a 3% NaCl solution. The results showed an important inhibition efficiency, about 96% for 4 h of testing time.

Keywords: 2-mercaptobenzimidazole; Electropolymerization; Insulating film

1. Introduction

In 1967, Ross and Kelly [1] obtained polypyrrole by electrochemical means for the first time. Since then, new polymers such as polyacetylene [3], polyparaphenylene, polythiophene and polyaniline [2] have been prepared electrochemically. Shirakawa et al. [3] have improvised an application for this type of polymer especially in the domain of protection against corrosion.

Organic coatings protect metals against corrosion by various mechanisms [4] that can be summarized as follows: (i) by suppression of the anodic and/or cathodic reaction, (ii) by the introduction of a high electrical resistance into the circuit of the corrosion cell, and (iii) as a barrier to aggressive species (oxygen, water, and ions).

The performance of organic coatings has been investigated through the evaluation of their barrier properties using electrochemical impedance spectroscopy (EIS). These properties have been evaluated by monitoring the uptake of water and ions into the coatings [4–9], and estimating the degree of coating delamination [10,11]. The uptake of ions has been related to a decrease in electrical coating resistance [4–7] while the uptake of water has been related to an increase in coating capacitance [8,9].

2. Experimental

The experiments were performed in a classical three-electrode electrochemical cell. The working electrode was a rotating disk consisting of cylindrical (60 Cu–Zn) samples and had a 1-cm^2 cross-sectional area. The samples were first polished with emery paper grade 1000 and rinsed with acetone. The auxiliary electrode was a large surface area platinum grid and an Ag/AgCl electrode was used as reference. All potentials presented are referred to this electrode.

The solution used to deposit polymer was constituted by:

2-mercaptobenzimidazole (monomer) — 98%, ACROS; potassium hydroxide (supporting electrolyte) — 85%, GPR; methanol (solvent) — 99.8%, SOCHILD.

The experiments were carried out at 20°C. The voltammograms, *I–t* transient curves and the electrochemical impedance measurements were performed using an EG & G potentiostat (model 6310) driven by a computer.

* Corresponding author. Laboratoire d'Electrochimie et des Etudes de Corrosion, Faculté des Sciences, Université IBM Tofail, BP 133, Kénitra, Morocco.

E-mail address: bassouli1@hotmail.com (B. Assouli).

0032-3861/01/$ - see front matter
PII: S0032-3861(00)00578-4

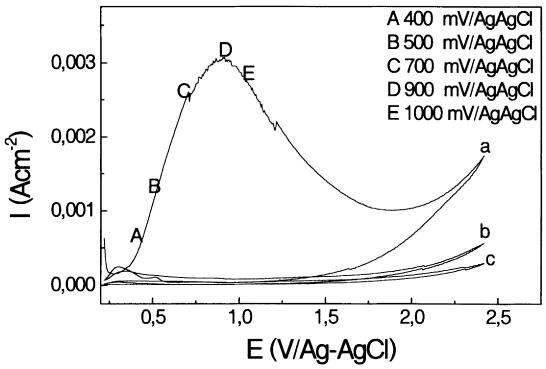

Fig. 1. Voltammograms of Cu–Zn substrate performed in methanol alkaline solution at a scan rate of 10 mV s^{-1}, pH = 12.5 and $T = 20°C$ with 2-MBI (0.1 M). (a) First cycle, (b) second cycle, and (c) third cycle.

3. Results and discussion

3.1. Electrochemical properties of 2-mercaptobenzimidazole

3.1.1. Cyclic polarization

In Fig. 1 typical voltammograms are presented. They are recorded on a Cu–Zn electrode for potentials ranging from 0.2 to 2.4 V in the presence of 2-MBI.

The obtained voltammograms show only one peak around $E = 1$ V. This peak may be assigned to the oxidation of the monomer.

As shown in Fig. 1, the density of the current decreases when the number of cycles increases. The final value after three cycles is 0.5 μA cm^{-2}, attributed to the film formation on the electrode surface. The film efficiency may be evaluated by the I_{p1}/I_{p2} ratio, where I_{p1} and I_{p2} are the peaks of the current for the first and the second cycle, respectively. This ratio was compared with those recorded for Pt, Fe and Cu electrodes [12], and we found that the inhibiting efficiency increases following the order Pt < Fe < Cu ≈ Cu–Zn. This is in agreement with work carried out by various authors showing that monomer is a remarkable corrosion inhibitor for copper [13].

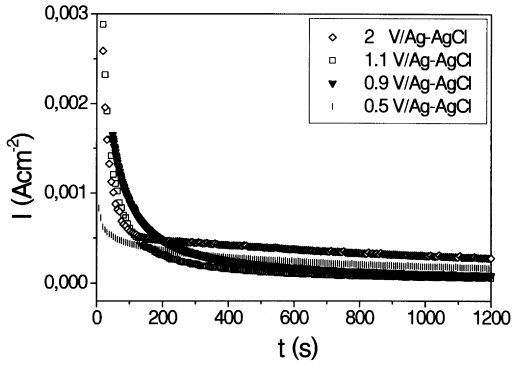

Fig. 2. Current–time curves of Cu–Zn substrate performed in methanol alkaline solution, at different potentials localized before and after the peak corresponding to the oxidation of the monomer.

3.1.2. Current–time curves

Fig. 2 shows the variation of the current density with time at different potentials localized before and after the peak corresponding to the oxidation of the monomer. A smooth current was observed while a thick polymer coating was formed. This improved the formation of the isolated organic layer on the electrode surface. The low value of the current obtained at the end of the electrolysis is attributed to the oxidation of the monomer through defect of the organic layer.

Current–time curves show that the homogeneous and adhesive film depends on the electrolysis potential value. At higher voltages, the fissured film is due to the oxidation of the electrolyte during the process of film formation [14]. At lower voltages, the film is formed but this requires a long time.

3.1.3. Electrochemical impedance

The impedance diagrams shown in Fig. 3 were obtained for a Cu–Zn electrode at different potentials localized before and after the peak corresponding to the oxidation of the monomer (Fig. 1). Two capacitive loops were observed.

The capacitance value for the high frequency (HF) loop varies between 4 and 10 μF cm^{-2}; this value is too low to correspond to a double layer (≈50 μF cm^{-2}). The associated parameters presented in Table 1 show that the product $R \times I$ (where R is the diameter of the capacitive time constant in the HF range and I is an anodic current density) is not constant, which makes it difficult to ascribe this loop to the charge transfer process.

These observations lead to the fact that the first time constant obtained on the impedance diagrams may be attributed to the charge transfer process coupled with a second process, which may correspond to mass transfer.

For lower frequencies, the value of capacity is lower than 1 mF cm^{-2}. This result could be explained either by the fact that the measured capacitance does not have the physical character of an interfacial one and/or by the presence of dissolution products on the metallic surface.

3.1.4. Scan rate

The influence of the scan rate on the cyclic voltammetry behavior of brass in the electropolymerization solution is shown in Fig. 4. The effect of scan rate (ν) on I_p and E_p characteristic of the oxidation monomer peak can be quantitatively analyzed (Table 2). Fig. 5 shows the relationship between I_p and $\nu^{1/2}$. The plot is in the form of a straight line with the ordinate at its origin equal to zero.

Additionally, it is also found that the E_p value for the peak shows a linear variation with logarithmic scan rate (Fig. 6). These findings suggest that the anodic processes, in the monomer oxidation potential range, are under diffusion control, and the corresponding system is completely irreversible [15].

The peak current I_p is related to the scan rate with relation

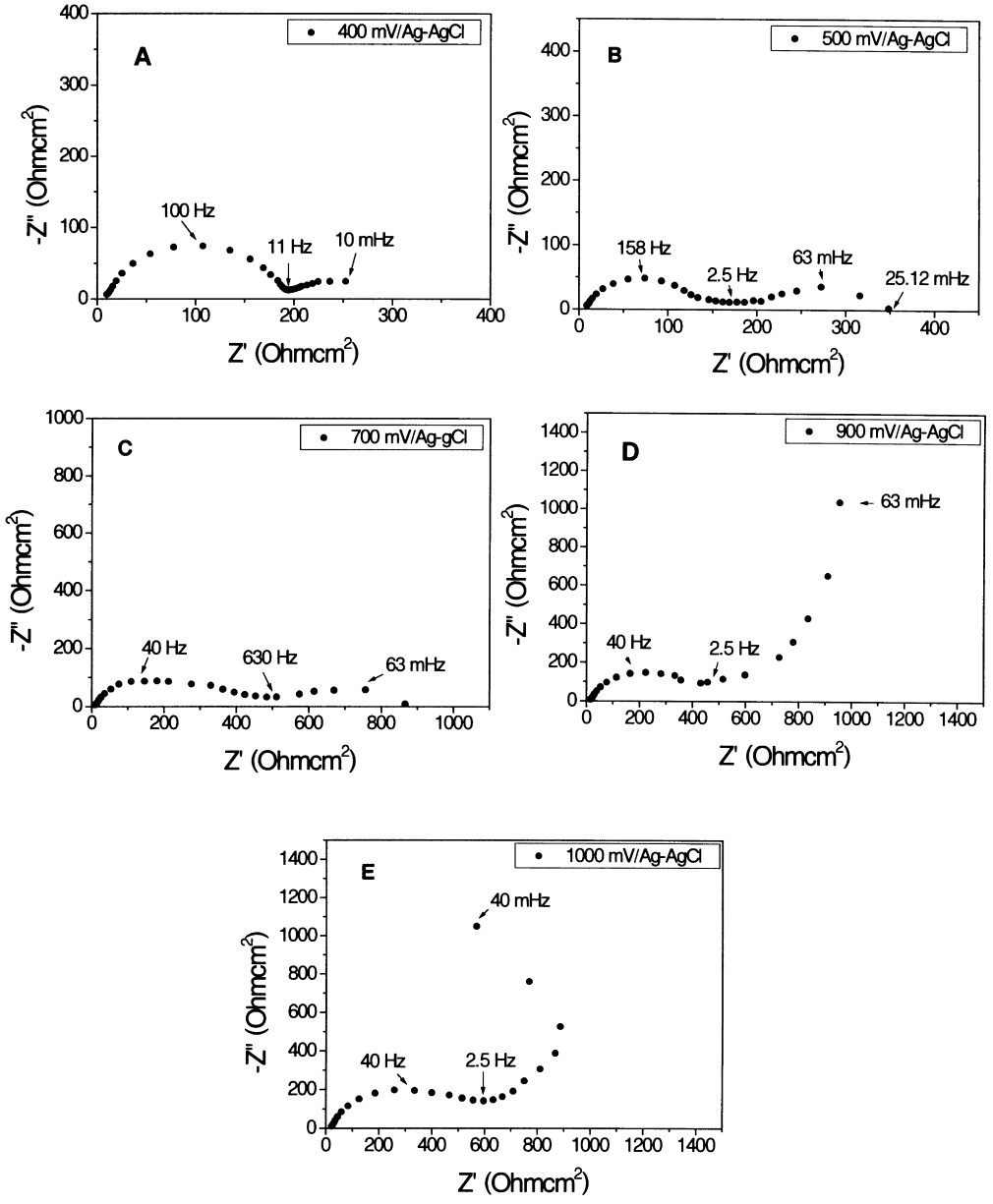

Fig. 3. Electrochemical impedance diagrams obtained on the Cu–Zn alloy at different potentials localized before and after the peak corresponding to the oxidation of the monomer.

[15,16]:

$$I_p = (2.99 \times 10^5) n(\alpha n_a)^{1/2} A C D_0^{1/2} \nu^{1/2}.$$

A, D_0, C, n, n_a, α and ν represent the electrode area, the diffusive species coefficient, the concentration of the diffusive species, the number of exchanged electrons, the apparent number of electrons transferred, the transfer coefficient and the scan rate, respectively.

Table 1
Effect of anodic polarization on HF parameters

Points	R_{HF} (Ω cm^2)	f_{HF} (Hz)	C_{HF} (μF cm^{-2})	$2.3R_{HF}I_A$ (mV)
A	187	100	8.5	115
B	135	185	7.5	184
C	264	63	9.5	483
D	429	39.81	9.3	621
E	588	39.81	7	667

The expression of the current of the peak becomes [15,16]

$$I_p = 0.227 nFAC_0 k^0 \exp\left[-\left(\frac{\alpha n_a F}{RT}\right)(E_p - E^0)\right]$$

This equation predicts that $\log(I_p)$ is linear vs. E_p with a slope equal to $-(\alpha n_a F/(RT))$, the electron transfer rate constant (k^0) can be calculated from the intercept (Fig. 7). We found: $E^0 = 287$ mV, $\alpha n_a = 0.55$, $k^0 = 5.57 \times 10^{-4}$ cm s^{-1} and $D_0 = 1.9 \times 10^{-8}$ cm^2 s^{-1}. Experiments were carried out using the conditions favored by Matsuda

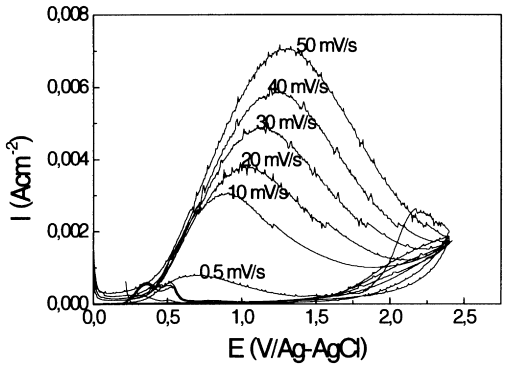

Fig. 4. Cyclic voltammograms of brass in electrodeposition medium at given scan rates, mV s^{-1}.

Table 2
Effect of scan rate on I_p and E_p

Scan rate (mV s^{-1})	I_p (mA cm^{-2})	E_p (mV)
10	3	907
20	3.7	1040
30	4.83	1139
40	5.86	1246
50	7	1318

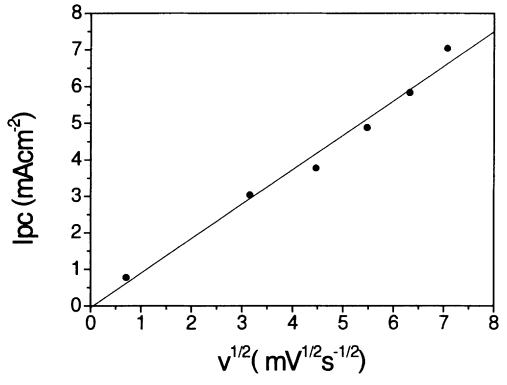

Fig. 5. Linear dependence of I_p on $\nu^{1/2}$ for brass in electrodeposition medium.

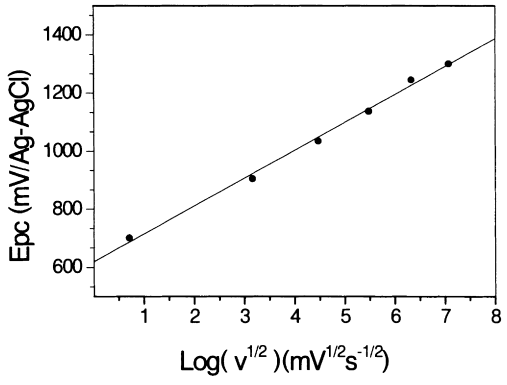

Fig. 6. Linear dependence of E_p on $\log(\nu^{1/2})$ for brass in electrodeposition medium.

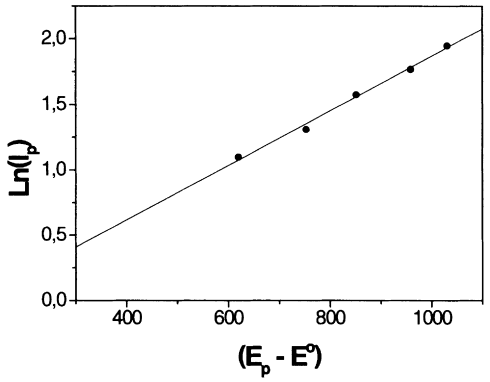

Fig. 7. Relationship between $\ln(I_p)$ and $(E_p - E^0)$ for brass in electrodeposition medium.

and Ayabe, i.e. $k^0 \leq 2 \times 10^{-5} \nu^{1/2}$cm s^{-1} [15,17]. The coefficient of the 2-MBI diffusive species found by this method is in agreement with the one found for copolymer polypyrrole–polyazulene (Ppy/Paz) [18].

3.2. Evaluation of corrosion resistance of poly(2-mercaptobenzimidazole) films in sodium chloride 3% solutions

The purpose of this study was to improve our understanding of the mechanism of protection offered by poly(2-MBI). Impedance measurements were performed as described earlier.

3.2.1. 3% NaCl solution

The impedance diagrams shown in Fig. 8 were obtained for the Cu–Zn electrode at E_{corr} in the absence of a polymeric film. Two capacitive loops were observed.

At low frequencies, the electrochemical impedance diagram is representative of charge transfer and mass transport. So, when the rotation speed increases, the polarization resistance decreases (Fig. 9). This effect was reversed in

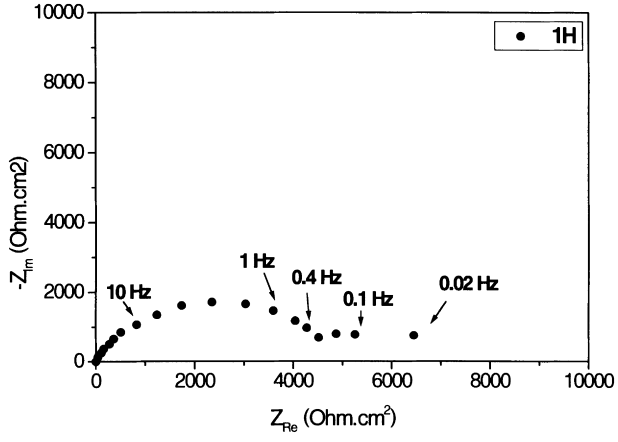

Fig. 8. Electrochemical impedance diagrams of brass in 3% NaCl obtained at E_{corr} after 1 h of immersion.

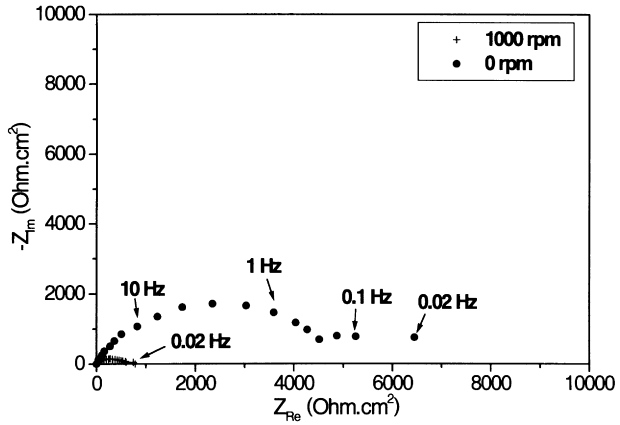

Fig. 9. Electrochemical impedance diagrams of brass in 3% NaCl determined for different rotation speeds after 1 h of immersion.

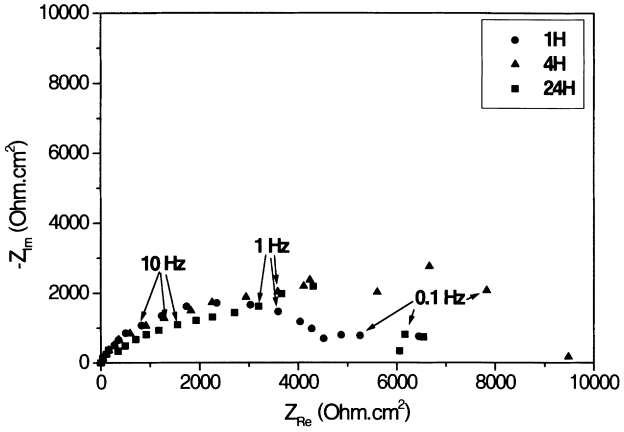

Fig. 10. Electrochemical impedance diagrams of brass in 3% NaCl determined for different immersion time.

view of the fact that immersion time increases (Fig. 10) indicating the diffusion through a porous layer of corrosion product [19–21].

At high frequencies, we have suggested that this loop was associated with a mixed kinetics because we cannot distinguish between the charge transfer and the diffusion process (the polarization resistance decreases when the rotation speed increases) (Fig. 9). In summary, the mass transport seems to take place in the corrosion processes of brass in 3% NaCl [22–24].

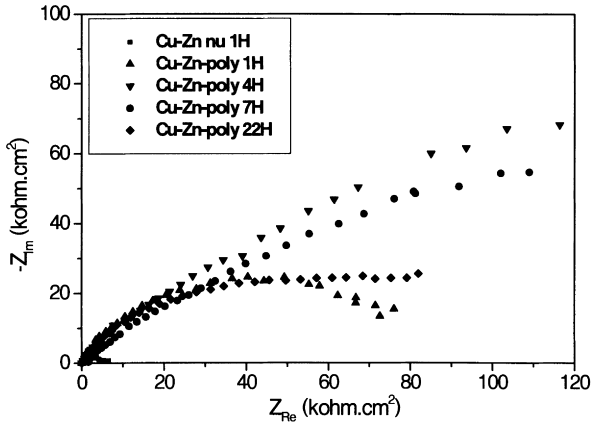

Fig. 12. Electrochemical impedance diagrams of brass with poly(2-MBI) coating in 3% NaCl determined for different immersion time.

3.2.2. Polymer coated metals

Application of models for the impedance behavior. Most authors agree that the simple AC impedance shown in Fig. 11 can be used for the analyses of impedance data for polymer coated metals that have been exposed to corrosive media [25–30]. At low frequencies we would expect to find the impedance response owing to the contact between the aqueous solution (at the bottom of the defects) and the metal. This concept of film porosity has been used recently by Walter [31].

Impedance data were interpreted using the equivalent electrical circuit of Fig. 11, where C_{film}, R_{film} and $f_{c(film)}$ represent the coating capacitance, the resistance related to the electrolyte passing through the coating defects and the characteristic frequency at the maximum of the imaginary part, respectively. According to Wong et al. [32] C_{dc} is the double layer capacitance, and R_{ct} is the charge transfer resistance.

In the present work, EIS of the polymer film formed on Cu–Zn electrodes was performed as a function of immersion time (Fig. 12). This is the typical behavior, which is expected from a metal-coating–electrolyte system. In the first hours of exposure to solution, the coating was slightly penetrated so that it presents predominantly a capacitive behavior. After 4 h of exposure, the diagram revealed a semicircle shape because the uptake of solution creates conductive pathways throughout the film, so that the system behaves like an association of capacitors and resistors. For

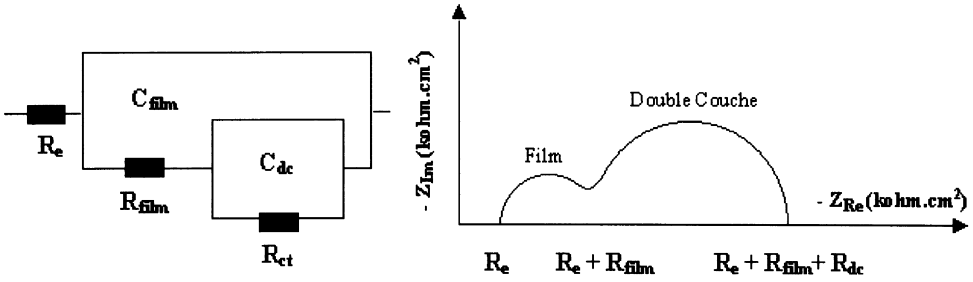

Fig. 11. Nyquist impedance spectrum of Cu–Zn/coating/NaCl 3% and the equivalent electrical circuit.

Table 3
Effect of brass electrode immersion time on characteristic parameters evaluated in high and low frequency ranges

t (h)	R_{film} (kΩ cm^2)	$f_{c(film)}$ (Hz)	C_{film} (μF cm^{-2})	R_{ct} (kΩ cm^2)	f_c (Hz)	C_{dc} (μF cm^{-2})
1	12	1.5	8.84	91	0.08	21.8
4	20	1	7.96	200	0.01	79.6
7	15	2	5.3	261	0.01	61
22	12	3.16	4.21	100	0.03	53.1

longer times the resistance decreases gradually as the film becomes more penetrated by the solution. However, for 22 h of exposure the resistance increases again owing to the start of reaction at the metal–polymer interface (Table 3).

4. Conclusions

The $I = f(E)$ and $I = f(t)$ permitted us to carry out the polymeric film properties as well as the optimal conditions of its formation. In this work, we have also studied the kinetics of electropolymerization of 2-MBI in methanol and alkaline solution by the EIS measurements.

The protective effect of organic coatings submitted to 3% NaCl solution has been evaluated. The results showed that the inhibition efficiency was very high (around 96% for 4 h of testing time).

References

[1] Ross SD, Kelly DJ. J Appl Polym Sci 1967;11:1209.
[2] Arsov LjD, Plieth W, Kobmehl G. J State Electrochem 1998;2:355–61.
[3] Shirakawa H, Louis EJ, Mac Diarmid AG, Chiang CK, Heeger AJ. J Chem Soc Chem Commun 1977:578.
[4] Bellucci F, Nicodermo L, Latanision RM. J Mater Sci 1990;25:1097.
[5] Deflorian F, et al. Corros Sci 1996;38:1697.
[6] Massiani Y, et al. Corros Sci 1993;34:1685.
[7] Popov BN, et al. J Electrochem Sci 1993;140:947.
[8] Van Westing EPM, et al. Corros Sci 1994;36:957.
[9] Van Westing EPM, et al. Corros Sci 1994;36:979.
[10] McCluney SA, et al. J Electrochem Soc 1992;139:1556.
[11] Van Weije DH, et al. Corros Sci 1994;36:643.
[12] Gi Xue, Huang X-Y, Dong J, Zhang J. J Electroanal Chem 1991;310:139–48.
[13] Kacemi A, Guenbour A, Ben Bachir A. Matér Tech 1997;1:47–54.
[14] Perrin FX, Pagetti J. Electrochem Meth Corros Res 1998;IV:440–6.
[15] Bard AJ, Faulkner LR. Electrochimie méthodes. Paris: Editions Masson, 1983.
[16] Ko JM, Rhee HW, Park SM, Kim CY. J Electrochem Soc 1990;137:139–48.
[17] Matcsuda H, Ayabe Y. Z Elektrochem 1955;59:494.
[18] Osaka T, Momma T. Electrochim Acta 1993;38(14):2011–4.
[19] Deslouis C, Triboullet B, Mengouli G, Musiani MM. J Appl Electrochem 1988;18:374.
[20] Feng Y, Teo W-K, Siow K-S, Tan K-L, Sieh A-K. Corros Sci 1986;38:369.
[21] Feng Y, Siow K-S, Teo W-K, Tan K-L, Sieh A-K. Corros Sci 1997;53:389.
[22] Duprat M, Dui N, Dabosi F. J Appl Electrochem 1978;8:455.
[23] Duprat M, Dabosi F. Corrosion 1981;37:89.
[24] Duprat M, Dabosi F, Moran F, Rocher S. Corrosion 1981;37:262.
[25] Leidheiser Jr. H. Corros Nace 1983;39:189–201.
[26] Walter GW. Corros Sci 1986;26:681–703.
[27] Keddam M, Takenouti H, Cetre Y, Diguet L. 8ème forum sur les impé. Electrochimiques, 1994. p. 163–73.
[28] Mansfled F. Evaluation of corrosion protection methods with electrochemical impedance spectroscopy. Corrosion 1987;481:1–23.
[29] Mansfled F. Electrochim Acta 1993;38(14):1891–7.
[30] Deflorian F, Fedrizzi L, Locaspi A, Bonora PL. Electrochim Acta 1993;38(14):1945–50.
[31] Walter GW. Corros Sci 1991;32(10):1041–103.
[32] Wong DKY, Coller BAW, MacFarlane DR. Electrochim Acta 1993;38:2121.